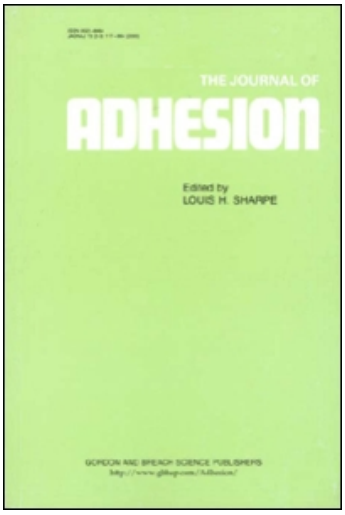

The Journal of Adhesion

Publication details, including instructions for authors and subscription information:
http://www.informaworld.com/smpp/title~content=t713453635

Estimation of Fatigue Strength for Adhesively-Bonded Lap Joints Based on Fatigue Failure Criterion Under Multiaxial Stress Conditions

Makoto Imanaka[a]; Takayoshi Iwata[b]
[a] Osaka University of Education, Asahigaoka Kashiwara City, Osaka, Japan [b] Research and Development Department, Toyoda Gosei Co. Ltd., Kitashima Inazawa City, Aichi, Japan

To cite this Article Imanaka, Makoto and Iwata, Takayoshi(1998) 'Estimation of Fatigue Strength for Adhesively-Bonded Lap Joints Based on Fatigue Failure Criterion Under Multiaxial Stress Conditions', The Journal of Adhesion, 65: 1, 7 — 24
To link to this Article: DOI: 10.1080/00218469808012236
URL: http://dx.doi.org/10.1080/00218469808012236

J. Adhesion, 1998, Vol. 65, pp. 7–24
Reprints available directly from the publisher
Photocopying permitted by license only

Estimation of Fatigue Strength for Adhesively-Bonded Lap Joints Based on Fatigue Failure Criterion Under Multiaxial Stress Conditions

MAKOTO IMANAKA[a,*] and TAKAYOSHI IWATA[b]

[a]*Osaka University of Education, Asahigaoka Kashiwara City, Osaka 582, Japan;*
[b]*Research and Development Department, Toyoda Gosei Co. Ltd., Kitashima Inazawa City, Aichi 492, Japan*

(Received 23 September 1996; In final form 3 February 1997)

A method for estimation of endurance limits for adhesively-bonded single and single-step double-lap joints was proposed which considers the stress multiaxiality in the adhesive layer. At first, fatigue tests and finite element analysis were conducted for these lap joints. Then, endurance limits of these joints were estimated using their stress distributions and critical regression equations which were obtained from the S-N data of adhesively-bonded scarf- and butterfly-type joints. The results indicate that the endurance limits of these lap joints can be estimated from the regression equation based on the maximum principal stress.

Keywords: Adhesively-bonded joints; fatigue strength; stress multiaxiality; life prediction; single-lap joint; single-step double-lap joint; finite element analysis

1. INTRODUCTION

Due to emphasis on design for minimum weight and need for joining different kinds of materials, *e.g.* ceramic/metal or FRP/metal, adhesive bonding is used to join several types of mechanical parts. To apply

*Corresponding author.

adhesively-bonded joints to mechanical structures more widely, it is necessary to define fracture criteria for the joints. Particularly, fatigue failure criteria are important for many mechanical parts are subjected to cyclic load *via* vibration and transmission of power. Hence, many studies have been performed on fatigue crack propagation behavior [1,2,3] and S-N relationship [4,5] of adhesively bonded joints. Furthermore, most adhesively-bonded joints have concentrated multiaxial stresses in the adhesive layer. Hence, fatigue failure criteria under multiaxial stress conditions are required for estimation of fatigue strength of adhesively-bonded joints. However, most studies regarding fatigue strength of adhesively-bonded joints have not addressed stress multiaxiality.

Two types of adhesively-bonded joints have considerably uniform multiaxial stress conditions in the adhesive layer under uniaxial loading conditions: adhesively-bonded scarf- and butterfly-type butt joints. Scarf joints have considerably uniform normal and shear stresses except at the free end of the adhesive layer, and their combination ratio can be varied by changing the scarf angle. However, it is difficult to realize conditions where the shear stress is dominant or the sole stress. Such a stress condition in the adhesive layer can be realized by using butterfly-type butt joints. Hence, in our previous work for obtaining a fatigue failure criterion under multiaxial stress conditions, fatigue tests were conducted for adhesively-bonded scarf- and butterfly-type butt joints [6]. The results indicated that at the endurance limit the maximum principal, the von Mises and the maximum shear stresses in the adhesive layer were correlated with the principal stress ratio.

In this study, a method for estimation of fatigue strength for adhesively-bonded single and single-step double-lap joints was proposed which considers the stress multiaxiality in the adhesive layer. At first, fatigue tests and finite element analysis were conducted for these lap joints. Endurance limits of these lap joints were then estimated using their stress distributions and the critical regression equation between endurance limit and the principal stress ratio obtained in our previous study [6]. Finally, these estimated endurance limits are compared with the experimental results.

2. EXPERIMENTAL METHOD AND ADHESIVELY-BONDED JOINT SPECIMENS

The shapes and sizes of the single and single-step double-lap joints are shown in Figure 1. As indicated in this figure, for both joints, the lap length was one of three values (20 mm, 30 mm, 40 mm), and the adhesive layer thickness was adjusted to 0.1 mm. The shapes and sizes of the scarf- and butterfly-type joints which were used to obtain fundamental fatigue data in our previous study [6] are also shown in Figure 2. The adherend and adhesive used in the lap, scarf and butterfly type butt joints were 0.5% C carbon steel (JIS. S55C) and a thermosetting structural epoxy adhesive (Toyoda Gosei: EA9432NA), respectively.

These adhesively-bonded joints were prepared as follows: The bonding surfaces of the adherends were polished with emery paper of

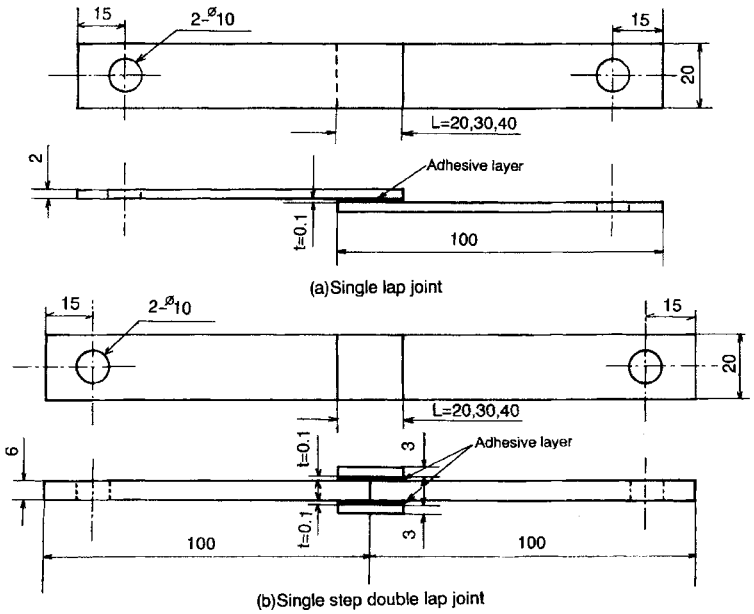

FIGURE 1 Shapes and sizes of the adhesively-bonded single- and single-step double-lap joints.

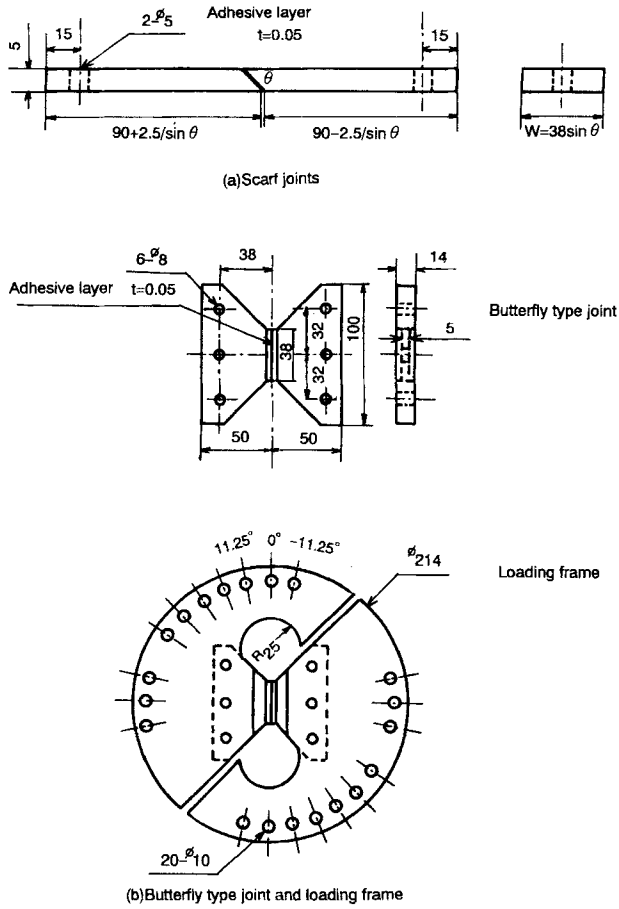

FIGURE 2 Shapes and sizes of the adhesively-bonded scarf- and butterfly-type joints.

grade 180 mesh under dry conditions. Then, the adherends were degreased with acetone in an ultrasonic bath. These adhesive joints were cured at 140°C for 1.5 hr and cooled in a furnace, and the spew fillet was removed carefully by use of an emery paper of grade 180 mesh, then allowed to stand for a day at room temperature and submitted to fatigue tests.

Cyclic tensile fatigue tests were conducted with an electro-hydraulic type fatigue testing machine under conditions of stress ratio $R = 0.1$ and loading frequency $H = 30$ Hz.

3. STRESS ANALYSIS

3.1. Stress Distributions

To investigate the stress distributions in the adhesive layer of these lap joints, two-dimensional stress analysis was conducted using the finite element code MARC, where plane strain condition was assumed. Young's modulus and Poisson's ratio of the adherend were 200 GPa and 0.319, respectively, and the corresponding adhesive properties were 4.3 GPa and 0.291, respectively. The boundary conditions of the single and single-step double-lap joints are shown in Figures 3(a) and (b), respectively.

Figure 4 shows the distributions of the maximum principal stress, σ_1, the maximum shear stress, τ_{max}, and the Mises equivalent stress,

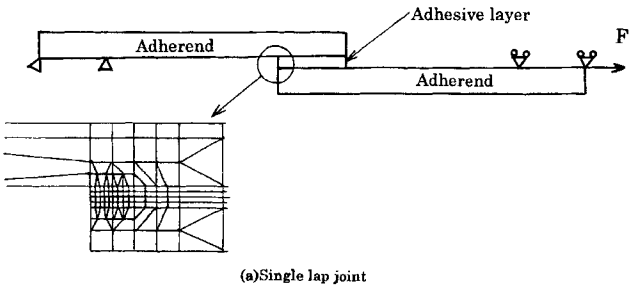

(a)Single lap joint

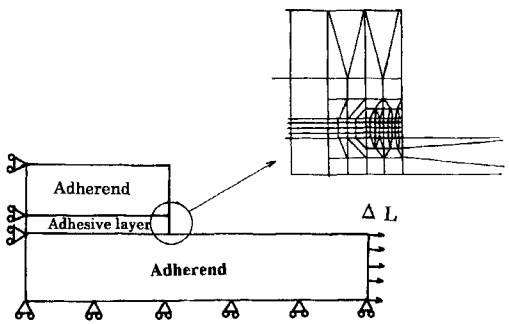

(b)Single step double lap joint

FIGURE 3 Boundary conditions and examples of mesh pattern near the lap end.

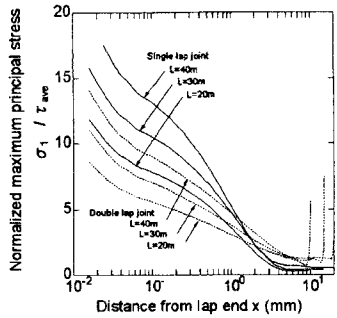

(a) Maxmum principal stress

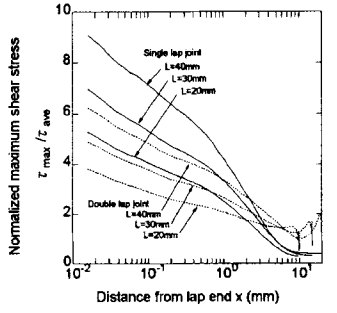

(b)Maximum shear stress

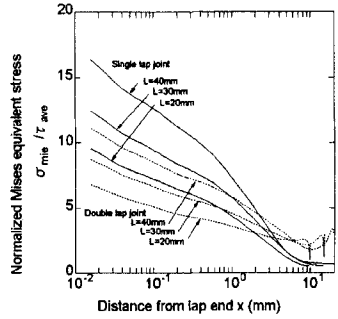

(c)Mises equivalent stress

FIGURE 4 Stress distributions of the single- and single-step double-lap joints.

σ_{mie}, along the adhesive/adherend interface for both lap joints by taking the lap length as a parameter, where the interfacial stress was taken as the stresses of Gaussian integration points within the adhe-

sive layer nearest to the interface. In this figure, the value on the abscissa is the distance from the lap end, and that on the ordinate is normalized with the average shear stress, τ_{ave}, in the adhesive layer which is calculated by dividing the applied load by the bonding area.

As shown in this figure, since the lap ends are singularity points for the both lap joints, all normalized stresses rise rapidly near the free end. Furthermore, the normalized stresses near the lap end increase with lap length for both lap joints, and these stresses for the single-lap joint are higher than those for the single-step double-lap joint with same lap length. This is because the single-step double-lap joint is symmetrical with the loading axis, hence the bending moment of the lap end is lower than that of single-lap joints. This figure also indicates that the gradient of these distributions decreases with increasing distance from the lap end for all joints. In the middle of the joints, single-lap joints have considerably uniform stress distributions. However, all stress components of single-step double-lap joints rise rapidly near the middle of the joints.

3.2. Stress Multiaxiality

Generally, stress multiaxiality affects the mechanical properties of most polymeric materials [7]. Furthermore, most adhesive joints have concentrated multiaxial stresses in the adhesive layer. Hence, the stress multiaxiality in the adhesive layer should be taken into account for estimating strength of adhesively-bonded joints. In our previous study [6], the endurance limits of the scarf- and butterfly-type joints were evaluated using the principal stress ratio, σ_3/σ_1, where σ_1 and σ_3 were the maximum and minimum principal stresses, respectively.

Figure 5 shows the distributions of σ_3/σ_1 for both lap joints with various lap lengths. As shown in this figure, within 1 mm from the lap end σ_3/σ_1 of all joints decreases gradually with increasing distance from the lap end, but there are only small differences in σ_3/σ_1 between joint types and lap lengths. However, when the distance from the lap end is over 1 mm, σ_3/σ_1 for both lap joints rapidly decreases. Further increases of the distance lead to the minimum values for both joints.

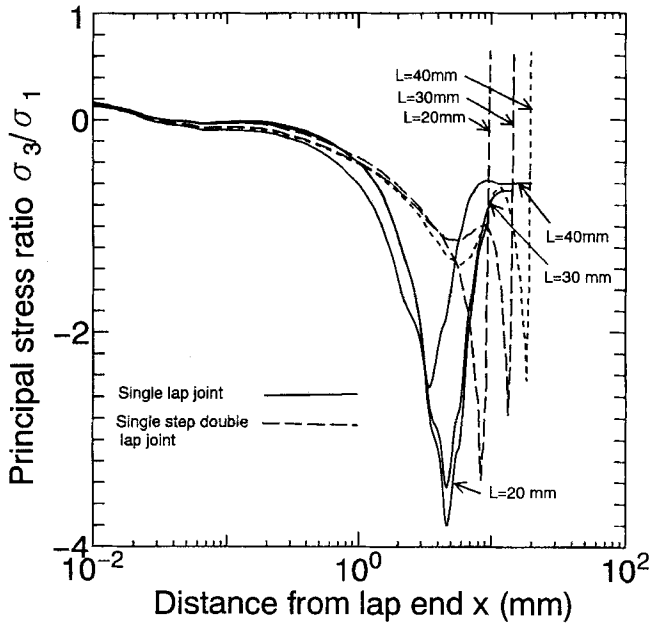

FIGURE 5 Distributions of the principal stress ratio for the single- and single-step double-lap joints.

4. RESULTS AND DISCUSSION

4.1. Results of Fatigue Tests

Figure 6 shows the relationship between load range, ΔL, and number of stress cycles of failure, N_f, for the both lap joints. As shown in this figure, the slopes of the $\Delta L - N_f$ relationships are gentle irrespective of the joint type and lap length. This trend means that the ratio of the fatigue propagation period to the total fatigue life is small. Furthermore, this figure also shows that fatigue strength increases with lap length for both joints, and the fatigue strength of the single-step double-lap joint is more than twice as high as that of the single-lap joint with the same lap length, although the adhesive area of the single-step double-lap joint is twice that of the single-lap joint with same lap length.

Based on Figure 6, the effects of lap length on the endurance limits at 10^7 for both lap joints are shown in Figure 7. In this figure, the endurance limits are indicated by the load range, ΔL_w, and average shear stress range, $\Delta\tau_w$, obtained by dividing load range, ΔL_w, by the bonding area. As shown in this figure, the slope of the $\Delta L_w - L$ curves for both lap joints decreases with increasing lap length. Hence, $\Delta\tau_w$ decreases with increasing lap length. Furthermore, $\Delta\tau_w$ of the single-step double-lap joint is over 30% of the single lap joint with the same lap length within the range from 20 mm to 40 mm.

4.2. Estimation of Endurance Limit

There are two methods to estimate the strength of adhesive joints with a singularity point at the free end. One is by using the stress-singularity parameter [8,9], and the other is based on the point stress criterion [10], *i.e.* the stress value at δ mm from the singularity point is critical for estimating joint strength. In this study, the endurance

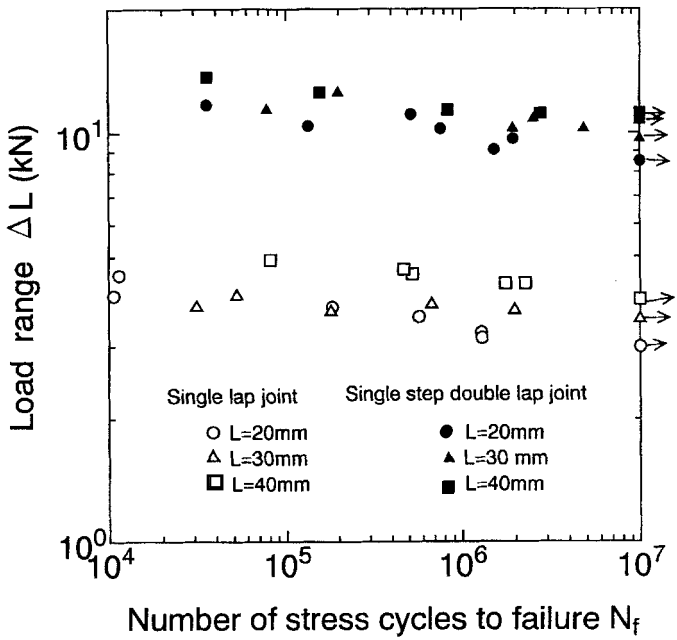

FIGURE 6 $\Delta L - N_f$ relationships of the single- and single-step double-lap joints.

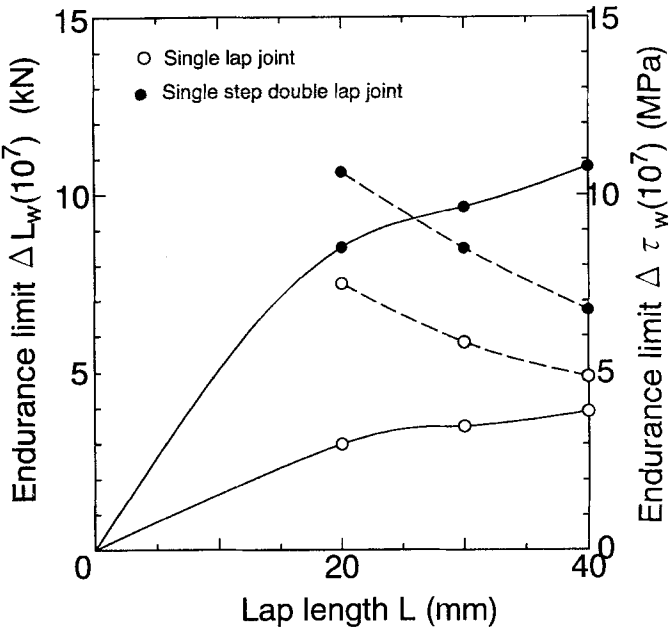

FIGURE 7 Effects of lap length on the endurance limit.

limits for both joints are tentatively estimated based on the point stress criterion.

Usually, when estimating a strength based on the point stress criterion, the critical strength, σ_f, is assumed to be constant as shown in Figure 8(a). However, as mentioned above, the stress multiaxiality affects the strength of the adhesive layer. Hence, we propose the modified model shown in Figure 8(b): the critical strength, σ_f, varies with the stress multiaxiality. In this case, σ_f corresponds to the critical endurance limit, and σ_w is determined by the principal stress ratio using regression equations, Eqs. (1)–(3), obtained in our the previous study [6].

$$(\sigma_1)_w = 37.88 - 10.88(\sigma_3/\sigma_1) \tag{1}$$

$$(\tau_{max})_w = 19.84 - 26.80(\sigma_3/\sigma_1) \tag{2}$$

$$(\sigma_{mie})_w = 35.43 - 44.87(\sigma_3/\sigma_1) \tag{3}$$

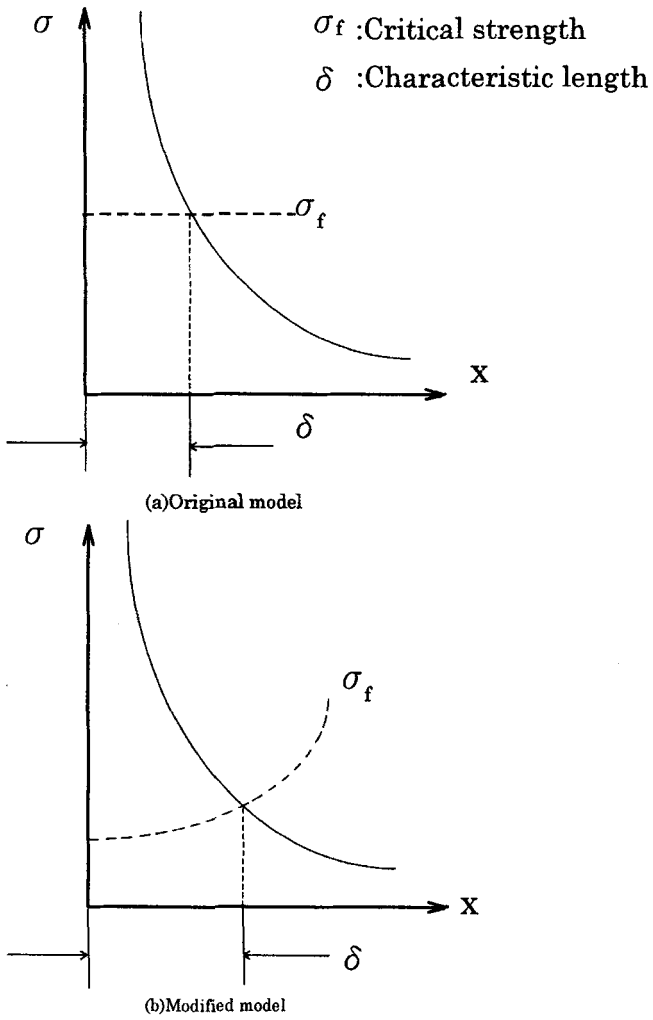

FIGURE 8 Point stress model.

where $(\sigma_1)_w$, $(\tau_{max})_w$ and $(\sigma_{mie})_w$ are the maximum principal, the maximum shear and the von Mises equivalent stresses at the endurance limit, respectively, and correlation coefficients of these equations were over 0.95.

Figures 9 and 10 show the distributions of stresses at the endurance limit and those of critical endurance limits for the single and single-

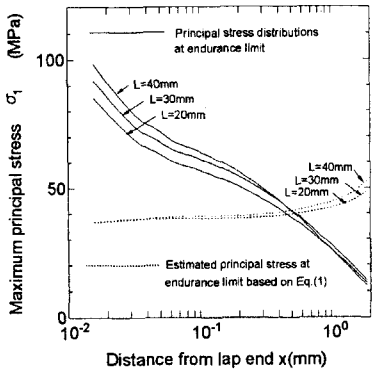

(a)Arranged by the maximum principal stress

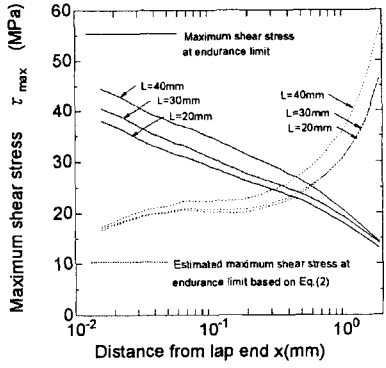

(b)Arranged by the maximum shear stress

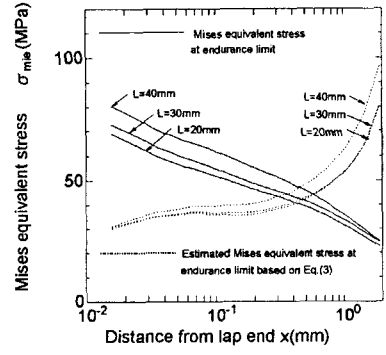

(c)Arranged by the Mises equivalent stress

FIGURE 9 Stress distributions of the single-lap joints at endurance limit.

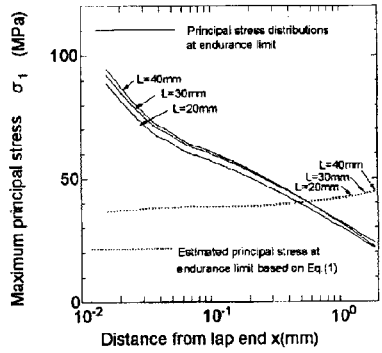

(a)Arranged by the maximum principal stress

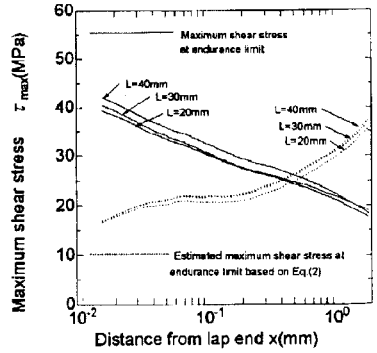

(b)Arranged by the maximum shear stress

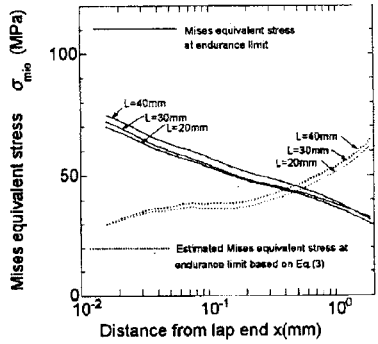

(c)Arranged by the Mises equivalent stress

FIGURE 10 Stress distributions of the single-step double-lap joints at the endurance limit.

step double-lap joints, respectively. In these figures, the solid lines indicate distributions of σ_1, τ_{max} and σ_{mie} at the endurance limit, and broken lines indicate critical endurance limits of these joints obtained by substituting σ_3/σ_1 for Eqs. (1)–(3), where the distributions of σ_3/σ_1 can be obtained from Figure 5.

As shown in Figures 9 and 10, both the solid and dashed lines for different lap lengths have narrow bands, where the width of these scatter bands indicates the degree of standardization. More detailed observation of these figures leads the following trends: The difference of the scatter band widths of both solid and dashed lines between single and single-step double-lap joints is small. However, the scatter band widths of both lines vary with the kind of stresses components for both the lap joints.

Besides, the absolute stress value varies with the kind of stress component. Hence, when comparing with the degree the standardization, the width of the scatter band should be evaluated by the relative band width which is divided by the absolute stress value. For both lap joints, it is confirmed that the relative band width of the solid and dashed lines arranged by the maximum principal stress are more narrow than those arranged by the maximum shear and von Mises equivalent stresses. This indicates that the maximum principal stress is a key parameter governing endurance limits for both lap joints.

Another parameter necessary for the estimation of endurance limit is the characteristic length, δ, which is obtained from the intersection point of corresponding solid and dashed lines as shown in Figure 8. For both lap joints, the characteristic length, δ, based on the maximum principal stress, ranges from 0.45 to 0.57, and the average characteristic length is 0.50 mm.

If a characteristic length is assumed, endurance limit can be estimated according to the flow chart indicated in Figure 11. At first, normalized maximum principal stress, σ_1/τ_{ave}, and the principal stress ratio, σ_3/σ_1 at $x = \delta$, can be obtained from Figures 4 and 5, respectively. Next, the critical endurance limit $(\sigma_1)_w$ at the point can be calculated by substituting the value of σ_3/σ_1 in Eq. (1). Then, the average shear stress range, $\Delta\tau_w$, at the endurance limit is obtained from the following equation.

$$\Delta\tau_w = (\sigma_1)_w/(\sigma_1/\tau_{ave}) \tag{4}$$

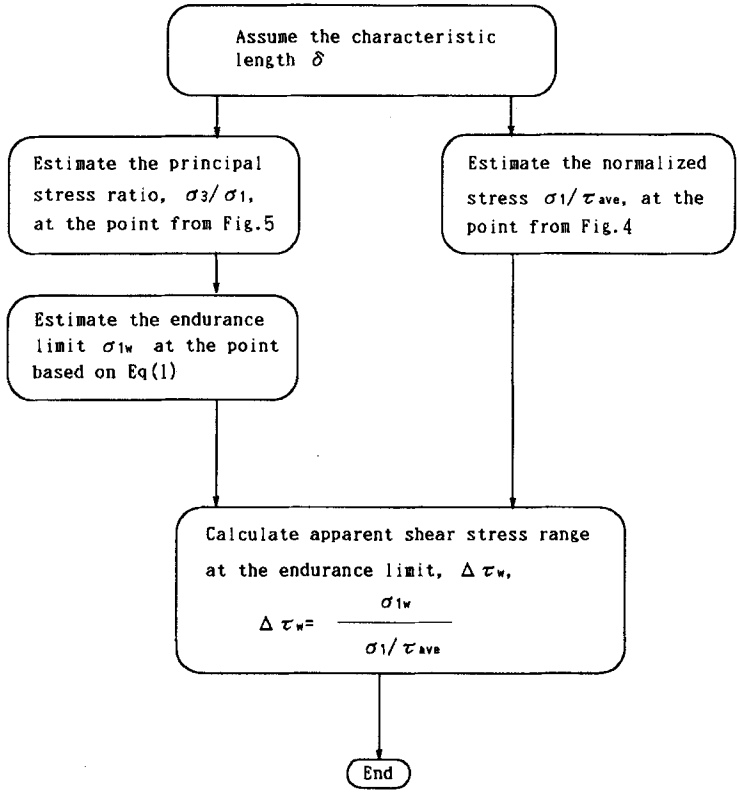

FIGURE 11 Flow chart for the estimation of the endurance limit.

Figure 12 shows the estimated endurance limits and experimental data for both lap joints, where the characteristic length, δ, is used for three cases, *i.e.*, 0.4 mm, 0.5 mm and 0.6 mm. The range of $\delta = 0.4 \sim 0.6$ mm is wider than that obtained from the intersection points of Figures 9 and 10, ranging $0.45 \sim 0.57$ mm. As shown in this figure, whereas δ is distributed over a wide range, all estimated lines are within the range 80% to 120% of the experimental data. Then, Figure 13 shows the difference between experimental data and estimated value of the endurance limits, where the abscissa represents a characteristic length, the ordinate being a normalized difference between experimental data and estimated value, which is obtained by dividing the difference by the experimental data. This figure shows

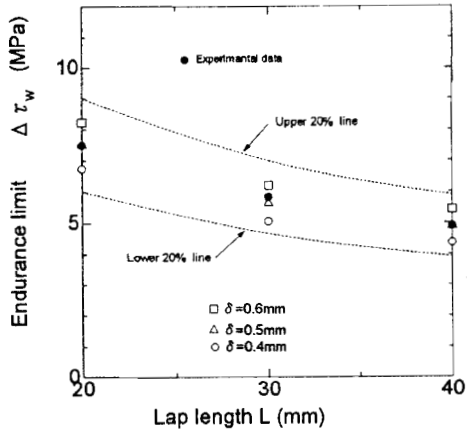

(a)Single lap joint

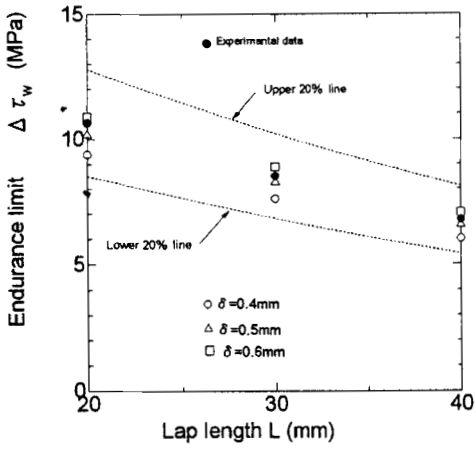

(b)Single step double lap joint

FIGURE 12 Estimated endurance limits based on the maximum principal stress.

that when $\delta = 0.5$ mm, the difference has a minimum value except for the single-step, double-lap joint with $L = 20$ mm. However, no correlation of the normalized difference with lap length or joint types is observed.

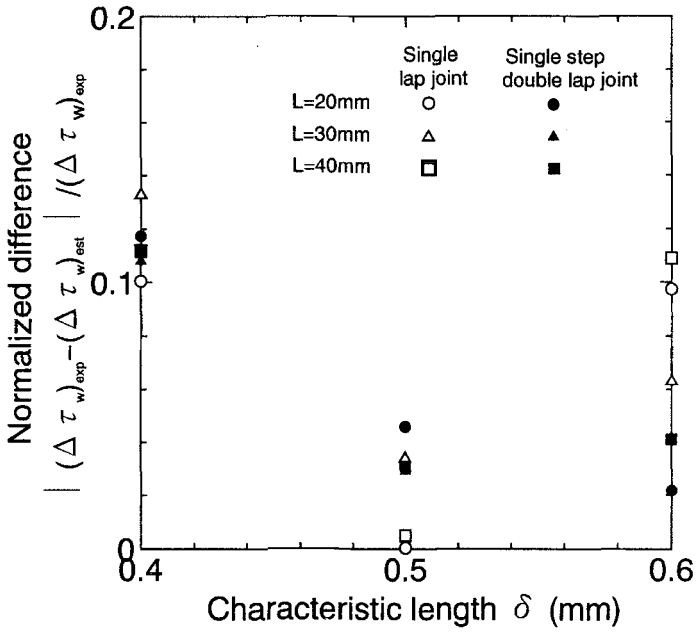

FIGURE 13 Effect of characteristic length on normalized difference between experimental data and estimated value.

5. CONCLUSIONS

Fatigue tests and finite element analysis were conducted for adhesively-bonded single- and single-step double-lap joints. Based on these results, the endurance limits of these lap joints were estimated using the stress distributions and the regression equations obtained in our previous study [6]. Major results obtained in this study are as follows:

(1) The normalized stresses near the lap end increased with lap length for both joints. Moreover, single-lap joints had higher normalized stress than single-step double-lap joints with the same lap length near the lap end.

(2) The total energy release rate of single-lap joints gradually increased with the crack length, whereas that of the single-step double-lap joints increased rapidly with crack length.

(3) Within 1 mm from the lap end the maximum principal stress ratio, σ_3/σ_1, of all joints decreased gradually with increasing distance from the lap end, but there are only small differences in σ_3/σ_1 between joint types and lap lengths.

(4) For both lap joints, the slopes of the $\Delta L - N_f$ relationships were gentle irrespective of lap length, and the apparent shear stress at the endurance limit, $\Delta\tau_w$, decreased with increasing lap length. Furthermore, $\Delta\tau_w$ for the single-step double-lap joint was over 30% as high as that of the single-lap joint within the range of lap length from 20 mm to 40 mm.

(5) The endurance limits for the single- and single-step double-joints were tentatively estimated based on the modified point stress criterion: The critical endurance limit, σ_w, was determined by using the regression equations obtained in our previous study and the distributions of σ_3/σ_1. It was confirmed that the endurance limits of these lap joints can be estimated with high accuracy from the regression equation based on the maximum principal stress, when the characteristic length, δ, is 0.5 mm.

References

[1] Dattaguru, B., Everett, R. A., Whitcomb Jr., J. D. and Johnson, W. S., *Trans. ASME J. Engineering Materials and Technol.* **106**, 59–65 (1984).
[2] Mall, S. and Johnson, W. S., **ASTM STP 893**, 322–334 (1986).
[3] Mall, S., Rezaizadeh, M. A. and Gurumurthy, R., *Trans. ASME J. Engineering Materials and Technol.* **109**, 17–21 (1987).
[4] Martin, R. H. and Sage, G. N., *Compos. Struct.* **8**, 141–163 (1986).
[5] Imanaka, M., Fukuchi, Y., Kishimoto, W., Okita, K., Nakayama, H. and Nagai, H., *Trans. ASME J. Engineering Materials and Technol.* **110**, 350–354 (1988).
[6] Imanaka, M. and Iwata, T., *J. Adhesion* **59**, 111–126 (1996).
[7] Nielsen, L. E., *Mechanical Properties of Polymers and Composites* (Marcel Dekker, Inc., New York, 1975).
[8] Rao, A. K., *ZAMM* **51**, 395–406 (1971).
[9] Hattori, T., *Japan Soc. Mech. Engineering Internat. J. Ser. I* **34**, 326–331 (1991).
[10] Whitney, J. M. and Nuismer, R. J., *J. Compos. Mater.* **8**, 253–265 (1974).